J. Fluid Mech. (2012), *vol.* 694, *pp.* 352–370. © Cambridge University Press 2012
doi:10.1017/jfm.2011.551

Steady free surface flows induced by a submerged ring source or sink

T. E. Stokes[1], G. C. Hocking[2]† and L. K. Forbes[3]

[1] Department of Mathematics, University of Waikato, Hamilton 3240, New Zealand

[2] Mathematics and Statistics, Murdoch University, Perth, WA 6150, Australia

[3] School of Mathematics and Physics, University of Tasmania, Hobart, TAS 7001, Australia

(Received 7 January 2011; revised 29 July 2011; accepted 14 December 2011;
first published online 24 January 2012)

The steady axisymmetric flow induced by a ring sink (or source) submerged in an unbounded inviscid fluid is computed and the resulting deformation of the free surface is obtained. Solutions are obtained analytically in the limit of small Froude number (and hence small surface deformation) and numerically for the full nonlinear problem. The small Froude number solutions are found to have the property that if the non-dimensional radius of the ring sink is less than $\rho = \sqrt{2}$, there is a central stagnation point on the surface surrounded by a dip which rises to the stagnation level in the far distance. However, as the radius of the ring sink increases beyond $\rho = \sqrt{2}$, a surface stagnation ring forms and moves outward as the ring sink radius increases. It is also shown that as the radius of the sink increases, the solutions in the vicinity of the ring sink/source change continuously from those due to a point sink/source ($\rho = 0$) to those due to a line sink/source ($\rho \to \infty$). These properties are confirmed by the numerical solutions to the full nonlinear equations for finite Froude numbers. At small values of the Froude number and sink or source radius, the nonlinear solutions look like the approximate solutions, but as the flow rate increases a limiting maximum Froude number solution with a secondary stagnation ring is obtained. At large values of sink or source radius, however, this ring does not form and there is no obvious physical reason for the limit on solutions. The maximum Froude numbers at which steady solutions exist for each radius are computed.

Key words: critical layers, surface gravity waves, wave breaking

1. Introduction

The flow generated during the withdrawal of fluid through a submerged outlet from a density-stratified reservoir, cooling pond or lake is of great importance to determining the quality of water for town supply or irrigation, and also in general management of the water body (see Imberger & Hamblin (1982)). The tendency for the withdrawal to occur in layers is known as selective withdrawal and the height of the withdrawal region is determined by the flow rate, degree of density stratification

† Email address for correspondence: G.Hocking@murdoch.edu.au

https://doi.org/10.1017/jfm.2011.551 Published online by Cambridge University Press

and geometry of the outlet. The problem can be broken into two general categories; continuous stratification and layered stratification. This paper is concerned with the latter. A review of work on the former can be found in Imberger & Patterson (1990).

The withdrawal from a fluid consisting of two layers of different densities or a single fluid with a free surface has been studied since the work of Sautreaux (1901), who obtained an exact solution, at a single flow rate, to the problem in which the water surface is pulled down into a cusp shape (see figure 1) directly above a line sink sitting atop a 'mountain' with a 120° angle at its apex. This solution has been reproduced in various guises by Craya (1949) and Tuck (1975). The cusp shape was believed to represent the critical transition (the so-called *critical drawdown*) between a single-layer flow and a two-layer flow, in which both layers are being withdrawn (see figure 1), e.g. air is also drawn into the sink in the case of an air–water interface. Peregrine (1972) computed asymptotic single-layer solutions at low flow rates which had a stagnation point on the free surface directly above the sink (see figure 1). Cusped solutions in more general geometries for withdrawal through a line sink were found by Tuck & Vanden Broeck (1984), Hocking (1985) and Vanden Broeck & Keller (1987), while Vanden Broeck, Schwartz & Tuck (1978) and Mekias & Vanden-Broeck (1991) and Forbes & Hocking (1993) computed further solutions with a stagnation point on the free surface. Vanden Broeck & Keller (1987) found many solutions with a cusp shape in a fluid of finite depth, but in all cases the situation with a fluid of infinite depth gave cusp solutions at a unique flow rate, e.g. Tuck & Vanden Broeck (1984).

A number of experimental investigations by Huber (1960), Harleman & Elder (1965), Wood & Lai (1972), Jirka (1979), Jirka & Katavola (1979) and Hocking (1991) observed that although the slow flows did indeed have a stagnation point like the solutions of Peregrine (1972), the critical drawdown flow rates seemed to be lower than for the cusped solutions. However, these experiments were performed with a diffuse interface between the layers and the effect of this is thought to decrease the critical value (Hocking 1991). In the two-dimensional case, a gap was found between the maximum flow rates at which solutions with a stagnation point and solutions with a cusp were obtained. In the corresponding three-dimensional axisymmetric case of flow into a point sink, attempts to compute cusp-like solutions (Forbes & Hocking 2003) met with limited success, with such solutions only found over a narrow range in parameter space.

Forbes & Hocking (1990) and Forbes, Hocking & Chandler (1996) and Hocking, Vanden Broeck & Forbes (2002) considered the steady axisymmetric flow into a point sink submerged beneath a free surface in semi-infinite and finite-depth fluid domains. It was found that there is a maximum flow rate at which steady solutions exist that corresponds to the formation of a stagnation ring on the free surface. On the other hand, the flow configuration due to a line sink was also found to have limiting maximal flows with a stagnation point above the sink, but no secondary stagnation point was found in the solutions. In fact, there was no obvious reason for the breakdown of the solutions. However, when surface tension was included in the problem by Forbes & Hocking (1993), a fold in the parameter space led to multiple solutions and a maximum flow rate beyond which no solutions could be obtained. The conclusions that can be drawn from these results for withdrawal flows are complicated by the fact that in the case of steady flow, the equations are identical for source and sink flows (due to the quadratic term in velocity in the free surface condition). Thus, the steady solutions may theoretically arise from either an unsteady source flow or an unsteady sink flow.

https://doi.org/10.1017/jfm.2011.551 Published online by Cambridge University Press

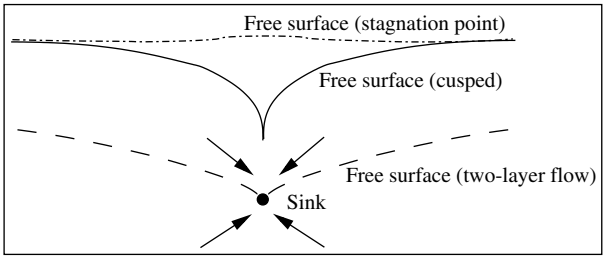


FIGURE 1. Schematic of free surface (or interface) shapes of the three steady flow types – stagnation point, cusped and two-layer. In the two-layer case, both layers of fluid are being withdrawn while in the other two situations flow only occurs in one layer.

Some of the uncertainty regarding critical drawdown of the free surface for flow into a line sink was resolved by Hocking (1995) and Hocking & Forbes (2001), who computed two-layer supercritical flows (see figure 1). They found that as the flow rate was reduced the limiting two-layer flow approached the single-layer cusped-surface solutions, seeming to verify that the cusped solutions are indeed the critical transition point.

Advances in computational techniques and power have allowed a consideration of unsteady motion due to the initiation or variation in strength of a submerged source or sink. Tyvand (1992) performed an analysis for small time, while Lubin & Springer (1967) and Xue & Yue (1998) did numerical calculations. More recently, Stokes, Hocking & Forbes (2002) and Stokes, Hocking & Forbes (2005) performed detailed computations to determine the critical drawdown values for withdrawal into both line and point sinks. It was shown that while there is some relation between the steady and unsteady flows, it is not always simple and direct. For example, it is not simply the case that a constant flow rate will progress through some unsteady flow history before settling into a steady state. In fact, it has been shown that there are a number of possible outcomes including non-uniqueness in parameter space, jet and splash formation and multiple critical drawdown values depending on flow history. Furthermore, the time-dependent problem does have a difference between source and sink flows, and source flows were generally found to be more stable (Stokes *et al.* 2002).

This rather confusing set of outcomes from previous work has led us to pursue this work further, initially in the steady case only. In this paper, we consider the steady flow due to a submerged ring sink or source beneath a free surface. The rationale for this is twofold. Firstly, it provides a simple manner of introducing a different geometry into the problem. Secondly, this flow has the interesting property that as the sink radius approaches zero the limiting behaviour should be that of a point sink and as the radius approaches infinity it should behave locally like a line sink. This interesting transition should provide insight into the differences between the two limiting cases.

We begin with a consideration of the asymptotic axisymmetric equations of steady flow into a ring sink. The solution of these equations suggests that if the ratio of sink radius to sink depth is less than $\sqrt{2}$, a single stagnation point forms on the free surface, while above this value both a stagnation point and a stagnation ring form. This result is proven in the low-flow limit. Further, it is possible to show that as the ring sink radius becomes large the solution approaches that of the flow due to a line sink. In the limit as the radius approaches infinity, the stagnation ring becomes the stagnation line above the 'line' sink. A numerical scheme is used to verify these

https://doi.org/10.1017/jfm.2011.551 Published online by Cambridge University Press

results and examine the full range of steady flows where the flow rate is no longer restricted to small values. Solutions are obtained at the limiting maximum values of the flow rate for each sink radius and the results are compared with earlier work.

2. Problem formulation

We consider the steady irrotational axisymmetric flow of an inviscid incompressible fluid beneath a free surface. The flow is driven by a line source or sink of strength m in a circular configuration, oriented horizontally beneath the free surface. The radius of this 'ring sink' is R and the depth beneath the undisturbed (with no flow) surface is H. Including these assumptions, the problem can be formulated in terms of a velocity potential $\phi(r, z)$, where r is a radial coordinate centred in the middle of the ring sink and z is the vertical coordinate with $z = 0$ corresponding to the level of the free surface if there is no flow.

Non-dimensionalizing the potential and length with respect to $(m/4\pi H)$ and H, respectively, where the quantity m is the total flux from the full ring sink, the problem is to solve

$$\nabla^2\phi = 0, \quad z < \eta(r), \quad (r, z) \neq (\rho, -1), \tag{2.1}$$

where $\rho = R/H$ is the non-dimensional sink radius, subject to

$$\tfrac{1}{2}(u^2 + v^2) + F^{-2}\eta = 0 \quad \text{on } z = \eta(r) \tag{2.2}$$

and

$$\phi_r\eta_r - \phi_z = 0 \quad \text{on } z = \eta(r). \tag{2.3}$$

Note that these equations include the main parameter that controls such flows, the Froude number

$$F = \left(\frac{m^2}{16\pi^2 g H^5}\right)^{1/2}, \tag{2.4}$$

in which g is gravitational acceleration. In most cases this can be thought of as an effective flow rate.

The velocity potential for a ring sink of radius ρ centred at $(x, y, z) = (0, 0, -1)$, i.e. located on $(x, y, z) = (\rho\cos\theta, \rho\sin\theta, -1)$, $0 \leqslant \theta < 2\pi$, in an unbounded fluid is given by the integral

$$\Phi_S = \frac{1}{2\pi\rho}\int_0^{2\pi} \frac{\rho}{\left[(x - \rho\cos\theta)^2 + (y - \rho\sin\theta)^2 + (z + 1)^2\right]^{1/2}}\,\mathrm{d}\theta. \tag{2.5}$$

The coefficient $1/(2\pi\rho)$ is to ensure the total flux is the same as for a single point sink, enabling easier comparison. A change of sign reverses the flow direction from a sink flow to a source flow. However, in the case of steady flow, the quadratic nature of the velocity term in the dynamic condition (2.2) means that solutions generated apply for both source and sink flows. Letting $x = r\cos\beta$, $y = r\sin\beta$ and simplifying, we get

$$\Phi_S(r, \theta, z) = \frac{1}{2\pi}\int_0^{2\pi} \frac{1}{\left[r^2 + \rho^2 + (z + 1)^2 - 2r\rho\cos\theta\right]^{1/2}}\,\mathrm{d}\theta. \tag{2.6}$$

https://doi.org/10.1017/jfm.2011.551 Published online by Cambridge University Press

Therefore, it is required that as $(x, y, z) \to (\rho\cos\theta, \rho\sin\theta, -1)$ for $0 \leqslant \theta < 2\pi$,

$$\phi(x, y, z) \sim \Phi_S. \tag{2.7}$$

3. Asymptotic solution for small flow rate

In this section, we obtain a leading order asymptotic steady-state solution for the potential function, ϕ, for small Froude number, F, depending on the radius ρ of the submerged ring source or sink. This leads to an $O(F^2)$ approximation for the shape of the free surface. Unfortunately, we cannot find a simple analytic form, but we can still glean useful information.

Assuming a small disturbance to the free surface, we must solve (2.1) subject to (2.2) and (2.3). Letting

$$\eta(r) = F^2\eta_1(r) + F^4\eta_2(r) + \cdots \tag{3.1}$$

and

$$\phi(r, z) = \phi_0(r, z) + F^2\phi_1(r, z) + \cdots \tag{3.2}$$

and expanding in z about $z = 0$, substituting into (2.3) and retaining terms of leading order gives

$$\phi_z = 0 \quad \text{on } z = 0, \tag{3.3}$$

and similarly (2.2), taking into account (3.3), gives

$$\eta_1(r) = -\tfrac{1}{2}\phi_{0r}^2(r, 0) \quad \text{on } z = 0. \tag{3.4}$$

Analogously to the point sink case in Stokes *et al.* (2005), we now define

$$\phi_0(r, z) = \frac{1}{2\pi}\int_0^{2\pi} \frac{1}{\left[r^2 + \rho^2 + (z+1)^2 - 2r\rho\cos\theta\right]^{1/2}}\,\mathrm{d}\theta + \frac{1}{2\pi}\int_0^{2\pi} \frac{1}{\left[r^2 + \rho^2 + (z-1)^2 - 2r\rho\cos\theta\right]^{1/2}}\,\mathrm{d}\theta. \tag{3.5}$$

This choice satisfies Laplace's equation and the limiting condition (2.7) as $(r, z) \to (\rho, -1)$, and represents a ring sink and its image reflected in $z = 0$. It satisfies (3.3) by the method of images, as we can see by differentiating (3.5) under the integral sign and setting $z = 0$. We can find the derivative with respect to r, giving

$$\phi_{0r}(r, 0) = \frac{1}{\pi}\int_0^{2\pi} \frac{-r + \rho\cos\theta}{\left(r^2 + \rho^2 + 1 - 2r\rho\cos\theta\right)^{3/2}}\,\mathrm{d}\theta, \tag{3.6}$$

and therefore the approximate surface shape is given by this result with (3.1) and (3.4).

3.1. *Stagnation ring formation*

While the solution in these variables is in a form that is easier to visualize from a physical point of view, it is in a slightly awkward form for analysis, and so we make a change of variable by setting $\bar{r} = r/\rho$, and using (3.4) gives $\bar{\eta}_1(\bar{r}) = -G(\bar{r})^2/(2\pi^2)$, where

$$G(\bar{r}) = \int_0^{2\pi} \frac{\bar{r} - \cos\theta}{\left(1 + \bar{r}^2 + \dfrac{1}{\rho^2} - 2\bar{r}\cos\theta\right)^{3/2}}\,\mathrm{d}\theta. \tag{3.7}$$

https://doi.org/10.1017/jfm.2011.551 Published online by Cambridge University Press

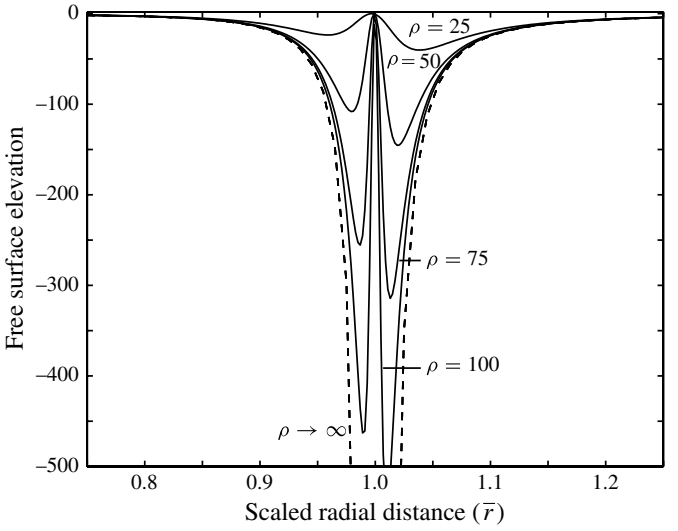


FIGURE 2. Asymptotic free surface shape, $\bar{\eta}(\bar{r})$, scaled so that the sink is always at $\bar{r} = 1$, with $\rho = 25, 50, 75, 100$ (and $\rho = \infty$ is dashed). In this non-dimensionalization, the sink depth increases at $\bar{r} = 1$ as ρ increases.

The sink/source is now always situated at $\bar{r} = 1$. In this modified form, ρ occurs in only one place and its effect can be more easily seen, in particular as it grows large, whereupon $\bar{\eta}_1(\bar{r})$ tends to

$$\bar{\eta}_1(\bar{r}) \to -\frac{1}{2\pi^2}\left(\int_0^{2\pi} \frac{\bar{r} - \cos\theta}{\left(1 + \bar{r}^2 - 2\bar{r}\cos\theta\right)^{3/2}}\,\mathrm{d}\theta\right)^2 \quad \text{as } \rho \to \infty. \tag{3.8}$$

After some algebra (see appendix A), we may write

$$G(\bar{r}) = \frac{2}{\bar{r}q}\left[\frac{(\bar{r}^2 - 1 - 1/\rho^2)}{p^2}E(\zeta) + K(\zeta)\right], \tag{3.9}$$

where $p = \sqrt{(1-\bar{r})^2 + 1/\rho^2}$, $q = \sqrt{(1+\bar{r})^2 + 1/\rho^2}$, $\zeta = 4\bar{r}\left[(1+\bar{r})^2 + 1/\rho^2\right]^{-1}$ and $K(\zeta)$ and $E(\zeta)$ are the complete elliptic integrals of the first and second kinds (see Abramowitz & Stegun 1970).

Note that in the limit as $\rho \to \infty$, the presence of the p and q terms in the denominator produces irremovable singularities and hence vertical asymptotes at $\bar{r} = \pm 1$, directly above the ring sink. However, for finite ρ, there are no vertical asymptotes.

For large ρ, something approximating the $\rho = \infty$ case is obtained, with the free surface developing a dip of decreasing relative width but increasing depth; see figure 2, where the asymptotic ($\rho \to \infty$) case appears as a dashed curve. Note that the ring sink is at depth ρ^2 in this non-dimensionalization, and so the maximal depth of the surface profile is actually decreasing as a fraction of the submergence depth of the ring sink.

Indeed, plotting $\bar{\eta}_1(\bar{r})$ for a range of different values of ρ shows that for $\rho \leqslant 1.41$, the steady state produced is qualitatively similar to the situation in the point-sink case $\rho = 0$: there is a single stagnation point at $\bar{r} = 0$, and then a stagnation point 'at infinity" in all directions (see figure 2). However, for $\rho \geqslant 1.42$, a stagnation ring inside $\bar{r} = 1$ exists, and has increasing prominence as ρ increases. This can clearly be seen

https://doi.org/10.1017/jfm.2011.551 Published online by Cambridge University Press

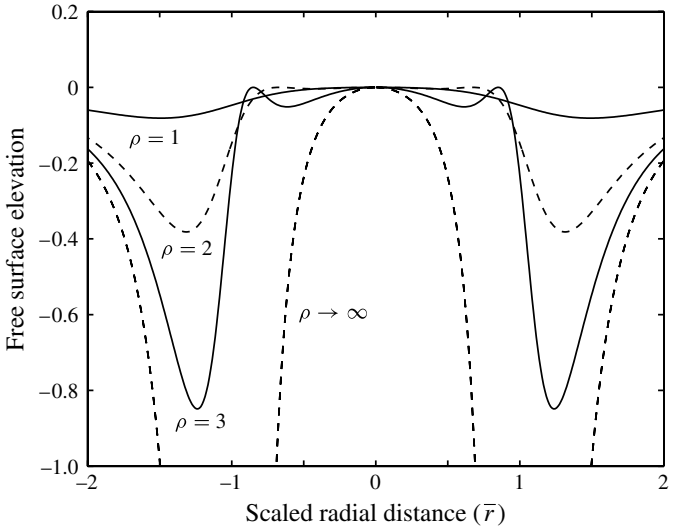


FIGURE 3. Asymptotic free surface shapes $\bar{\eta}(\bar{r})$, with $\rho = 1, 2, 3$ (and $\rho = \infty$ is dashed), showing the transition through the formation of the stagnation ring as ρ increases. At $\rho = 2$, the stagnation ring is only just becoming evident on an almost flat central region. The sink is at $\bar{r} = 1$ for all cases.

in figure 3, where the normalized variables $\bar{\eta}, \bar{r}$ are plotted against each other for $\rho = 1, 2, 3$, respectively. Examination of the solutions around this value reveals that the stagnation ring appears to be shed from the central stagnation point as ρ passes through $\rho = \sqrt{2}$ and then moves outward as ρ increases.

Careful calculation showed that the presence of the ring sink coincides to high accuracy with $\rho > \sqrt{2}$ and thus we conjecture the following theorem.

THEOREM 1. *The integral*

$$I = \int_0^{2\pi} \frac{\bar{r} - \cos\theta}{\left(1 + \bar{r}^2 + \dfrac{1}{\rho^2} - 2\bar{r}\cos\theta\right)^{3/2}} \, \mathrm{d}\theta \tag{3.10}$$

has two zeros if $\rho > \sqrt{2}$ *, namely* $\bar{r} = 0$ *and a second one for some* $\bar{r}$ *between* 0 *and* 1 *(and asymptotically close to* 1 *as* $\rho \to \infty$*), but only one zero if* $\rho < \sqrt{2}$ *, namely* $\bar{r} = 0$*.*

The proof of this theorem is provided in appendix B. Therefore, we have shown that if the ring sink has radius $\rho < \sqrt{2}$, then there is only a single central stagnation point in the linear solution, but if $\rho > \sqrt{2}$ a stagnation ring forms and moves outward as ρ increases (see figure 3).

3.2. *Limiting solution as* $\rho \to \infty$

It is also of interest to determine the behaviour of the asymptotic solution as the ring sink radius becomes large. In this limit, the ring sink solution should approach the asymptotic solution for low Froude number flow into a line sink.

https://doi.org/10.1017/jfm.2011.551 Published online by Cambridge University Press

Assume ρ is very large (but finite) and let $\epsilon = 1/\rho$, and write $1 - \bar{r} = k\epsilon$ for some fixed real k. Hence,

$$p = \epsilon\sqrt{k^2 + 1} \tag{3.11}$$

$$q = \sqrt{(2 - k\epsilon)^2 + \epsilon^2} = 2 - k\epsilon + O(\epsilon^2) \tag{3.12}$$

and

$$\zeta = \frac{4(1 - k\epsilon)}{(2 - k\epsilon)^2 + \epsilon^2} = 1 - (1 + k^2)\epsilon^2 + O(\epsilon^3). \tag{3.13}$$

Incorporating these into (3.9) and noting that as $m \to 1$, $K(m) \to (1/2)\ln(16/(1 - m))$ and $E(m) \to 1$ then after some work we see that as $\epsilon \to 0$ and $\zeta \to 1$,

$$G(\bar{r}) \sim \left(1 + \frac{3}{2}k\epsilon + O(\epsilon^2)\right)\left[-\frac{1}{\epsilon}\left(\frac{2k}{k^2 + 1}\right) + \ln\left(\frac{4}{\sqrt{1 + k^2\epsilon}}\right)\right], \tag{3.14}$$

which means that

$$G(\bar{r}) \sim -\frac{1}{\epsilon}\left(\frac{2k}{k^2 + 1}\right) + \ln\left(\frac{4}{\sqrt{1 + k^2\epsilon}}\right). \tag{3.15}$$

Now, since $\ln\epsilon/(1/\epsilon) \to 0$ as $\epsilon \to 0$ and $\eta_1(r) = -(1/(2\rho^4\pi^2))G(\bar{r})^2$, and noting that the equivalent two-dimensional Froude number is

$$F_2 = \frac{F}{2\pi\rho}, \tag{3.16}$$

we obtain to order F^2,

$$\begin{aligned}\eta(r) \approx F^2\eta_1(r) &= -\frac{8F_2^2}{\rho^2}\left[\frac{(1 - \bar{r})}{(1 - \bar{r})^2 + \dfrac{1}{\rho^2}}\right]^2 \\ &= -8F_2^2\left[\frac{\rho\overline{\delta r}}{(\rho\overline{\delta r})^2 + 1}\right]^2,\end{aligned} \tag{3.17}$$

where $\overline{\delta r} = 1 - \bar{r}$ is the horizontal distance from the ring sink. Therefore, in terms of the natural spatial variable $\delta r = \rho\overline{\delta r}$, we have

$$\eta(r) = -8F_2^2\frac{\delta r^2}{(\delta r^2 + 1)^2}. \tag{3.18}$$

This is the form of the asymptotic steady solution for a line sink situated at $x = 0, z = -1$ obtained in Forbes & Hocking (1993), if δr is replaced by x. This solution is symmetric about $\delta r = 0$, indicating in particular that the two dips on either side of the stagnation ring in the asymptotic ring sink solution tend to the same depth as $\rho \to \infty$.

https://doi.org/10.1017/jfm.2011.551 Published online by Cambridge University Press

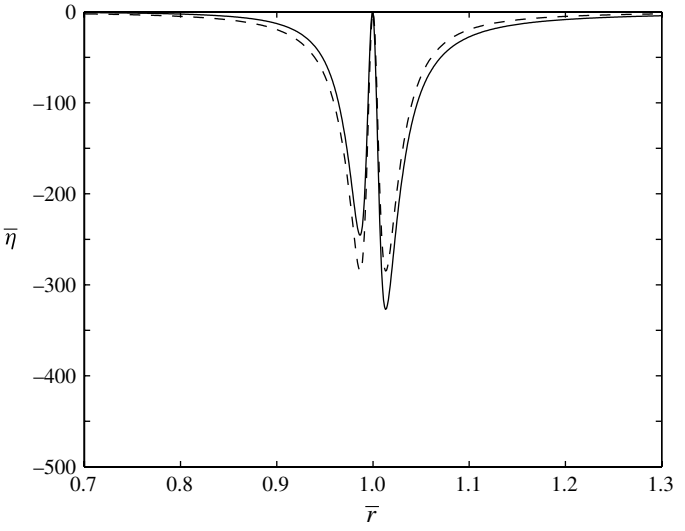


FIGURE 4. Large-ρ approximation to $\bar{\eta}(\bar{r})$, (3.19), with log term (graphically identical to (3.9)), with $\rho = 75$ (the rational approximation (3.18) is dashed).

3.3. *Supplement*

Note that by retaining the log term in (3.15), we obtain

$$G(\bar{r}) \sim \frac{-2(1-\bar{r})}{(1-\bar{r})^2 + \dfrac{1}{\rho^2}} + \ln\left(\frac{4}{\sqrt{\dfrac{1}{\rho^2} + (1-\bar{r})^2}}\right). \tag{3.19}$$

When this is substituted into $\bar{\eta}_1(\bar{r})$, although this is not formally valid, the result gives outstanding agreement with the general asymptotic solution for large ρ. In particular, the asymmetry in the dips on either side of $\bar{r} = 1$ is recovered (the rational term (3.18) is symmetric). Figure 4 shows $\bar{\eta}_1(\bar{r})$ for $\rho = 75$, computed directly from the form (3.9). The plot incorporating the log term is graphically indistinguishable from this solid curve. The single term consisting of the rational function (shown dashed) does not agree so closely. As ρ increases, the asymmetry reduces, and the two curves approach one another.

In terms of δr, this more accurate approximation has the form

$$\eta(r) \approx -2F_2^2\left[\frac{-2\delta r}{\delta r^2 + 1} + \frac{1}{\rho}\ln\frac{4\rho}{\sqrt{1+\delta r^2}}\right]^2. \tag{3.20}$$

4. The numerical method

In order to confirm the above results and to consider the full nonlinear steady flow problem, we performed a series of calculations using an approach similar to that of Forbes & Hocking (1990) and Hocking *et al.* (2002). The flow is again assumed to be axisymmetric and an integral equation is derived for the elevation and velocity potential on the free surface. We return to the use of the original non-dimensional variables, since these provide a clearer physical picture. The ring sink/source is of radius ρ and always at unit depth.

https://doi.org/10.1017/jfm.2011.551 Published online by Cambridge University Press

4.1. *Formulation*

The formulation of the numerical scheme follows almost exactly that given in Forbes & Hocking (1990), since the only difference between the two problems is the nature of the submerged singularity. The submerged point sink potential in Forbes & Hocking (1990) is replaced by the ring sink potential given by (2.6). However, for completeness, the method is summarized below.

We use Green's second identity to derive an integral equation for the unknown analytic function $\Phi(r, z)$ and surface elevation $z = \eta(r)$. Let Q be a fixed point on the free surface with coordinates $(r, \theta, \eta(r))$ and $P(\gamma, \beta, \mu)$ be another point which is free to move over the same surface. Since Φ is an analytic function over the full region except at the sink itself, we can define another function $\Psi = 1/R_{PQ}$ which is also analytic except when P and Q are the same point, i.e.

$$\Psi = \frac{1}{R_{PQ}} = \frac{1}{[r^2 + \gamma^2 - 2r\gamma\cos(\beta - \theta) + (z - \mu)^2]^{1/2}}, \tag{4.1}$$

so that we can invoke Green's second identity to obtain

$$\iint_{\partial V} \left[\Phi \frac{\partial \Psi}{\partial n} - \Psi \frac{\partial \Phi}{\partial n}\right] \mathrm{d}S = 0, \tag{4.2}$$

where n denotes the outward normal direction and ∂V consists of the surface of the free surface S_T, with the point Q carefully excluded by a small hemispherical surface, S_Q, a small sphere about the sink, S_ϵ, and the surface at infinity beneath the free surface, S_∞.

It is not difficult to show that the contributions from all of these surfaces lead to an integral equation of the form

$$2\pi\Phi(Q) = \int_0^{2\pi} \frac{\mathrm{d}\theta}{\left[r^2 + \rho^2 + (z+1)^2 - 2r\rho\cos\theta\right]^{1/2}} - \iint_{S_T} \Phi(P) \frac{\partial}{\partial n_P}\left(\frac{1}{R_{PQ}}\right) \mathrm{d}S_P, \tag{4.3}$$

where we note that the first term on the right-hand side is due to the ring sink with potential $2\pi\Phi_S$ from (2.6).

Equation (4.3) can also be written as

$$2\pi\Phi(Q) = 2\pi\Phi_S(Q) - \iint_{S_T} [\Phi(P) - \Phi(Q)] \frac{\partial}{\partial n_P}\left(\frac{1}{R_{PQ}}\right) \mathrm{d}S_P, \tag{4.4}$$

since (see Forbes & Hocking (1990))

$$\iint_{S_T} \frac{\partial}{\partial n_P}\left(\frac{1}{R_{PQ}}\right) \mathrm{d}S_P = 0. \tag{4.5}$$

This form turns out to be both accurate and stable numerically, enabling us to compute solutions until a critical F is reached.

Following Forbes & Hocking (1990), the surface integral can be specified in terms of the variables of the problem as

$$2\pi\Phi(Q) = 2\pi\Phi_S(Q) - \int_0^\infty (\Phi(P) - \Phi(Q)) K(a, b, c, d)\, \mathrm{d}\rho, \tag{4.6}$$

https://doi.org/10.1017/jfm.2011.551 Published online by Cambridge University Press

in which the kernel function is

$$\mathscr{K}(a,b,c,d) = \gamma \int_0^{2\pi} \frac{a - b\cos(\beta-\theta)}{[c - d\cos(\beta-\theta)]^{3/2}}\,\mathrm{d}\beta \tag{4.7}$$

and the four intermediate quantities a, b, c and d are defined as

$$a = \gamma\eta_\gamma(P) - (\eta(P) - \eta(Q)), \quad b = r\eta_\gamma(P), \tag{4.8}$$

$$c = \gamma^2 + r^2 + (\eta(P) - \eta(Q))^2, \quad d = 2r\gamma. \tag{4.9}$$

Forbes & Hocking (1990) reduced this to the form

$$\mathscr{K}(a,b,c,d) = \frac{2}{\sqrt{c+d}}\left[\eta_\gamma K\left(\frac{2d}{c+d}\right) + \left(\frac{2ar - \eta_\gamma c}{c-d}\right)E\left(\frac{2d}{c+d}\right)\right], \tag{4.10}$$

where K and E are the complete elliptic integrals of the first and second kinds as defined in Abramowitz & Stegun (1970). At this point, we note that E is well behaved over the interval of interest, but that K has a logarithmic singularity as $P \to Q$, in the integral over the free surface.

This problem was solved using a formulation based on arclength along the surface, so that s is the distance from $\gamma = 0$ to Q, and σ is the distance along the surface to P. The standard formula

$$\left(\frac{\mathrm{d}r}{\mathrm{d}s}\right)^2 + \left(\frac{\mathrm{d}\eta}{\mathrm{d}s}\right)^2 = 1 \tag{4.11}$$

defines the arclength s in terms of r and η. We define a surface potential $\phi(s)$ and, applying the chain rule, we find that along the surface,

$$\frac{\partial\phi}{\partial r} = \Phi_r(r,\eta) + \Phi_z(r,\eta)\frac{\mathrm{d}\eta}{\mathrm{d}r}. \tag{4.12}$$

Eliminating Φ_z from the Bernoulli equation (2.2) and the kinematic condition (2.3) and combining leads to a single relation,

$$\frac{1}{2}F^2\left(\frac{\mathrm{d}\phi}{\mathrm{d}s}\right)^2 + \eta(s) = 0, \tag{4.13}$$

on the free surface $z = \eta(r)$.

Rewriting the integral equation in terms of arclength, we obtain

$$2\pi\phi(s) = 2\pi\phi_S(s) - \int_0^\infty (\phi(\sigma) - \phi(s))\,\mathscr{K}(A,B,C,D)\,\mathrm{d}\sigma, \tag{4.14}$$

where

$$A = r(\sigma)\eta'(\sigma) - r'(\sigma)(\eta(\sigma) - \eta(s)), \quad B = r(s)\zeta'(\sigma), \tag{4.15}$$

$$C = r^2(\sigma) + r^2(s) + (\eta(\sigma) - \eta(s))^2, \quad D = 2r(s)r(\sigma). \tag{4.16}$$

This integral equation is coupled with the condition (4.11), subject to (4.13), to give the complete formulation of the problem. The arclength formulation would allow the method to find multiple-valued or overhanging free surface shapes if they exist.

4.2. *Computational details*

The equations derived in the previous section are highly nonlinear both because of the quadratic dependence on velocity of the surface condition and the fact that the

https://doi.org/10.1017/jfm.2011.551 Published online by Cambridge University Press

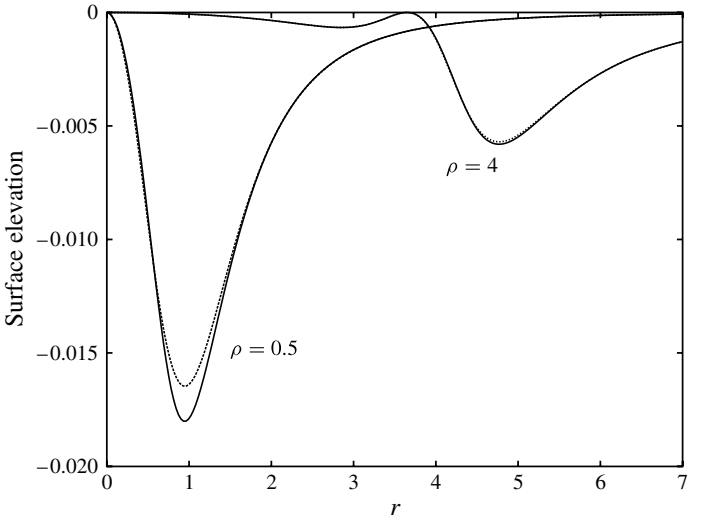


FIGURE 5. Comparison of the free surface shape computed from the asymptotic and nonlinear solutions for $F = 1.0, \rho = 4$ and $F = 0.3, \rho = 0.5$. The dashed lines are the asymptotic solutions.

surface shape is unknown. The equations were therefore solved numerically using collocation. A grid of points was chosen at arclength values $s = s_0, s_1, s_2, s_3, \ldots, s_N$. An initial guess for the surface shape $\eta = \eta_0, \eta_1, \eta_2, \ldots, \eta_N$ and potential function $\phi = \phi_0, \phi_1, \ldots, \phi_N$ was made and used to compute the error in the integral equation (4.14) and the condition on the surface (4.13). The initial guess was then updated using a damped Newton's method until the error in all equations dropped below 10^{-8}. In the paper by Forbes & Hocking (1990), (4.13) was used to find η once ϕ was 'known', halving the number of unknowns, and all integration was performed using cubic splines. In this work, both η and ϕ along the surface were treated as unknowns and integration using the trapezoidal rule was found to give solutions to graphical accuracy with a step of $\Delta s = 0.04$. This difference can in part be attributed to the significant increase in computational power since the publication of Forbes & Hocking (1990), in which $\Delta s = 0.04$ was used, but with truncation at only $s_N = 6.0$ and an absolute maximum of $N = 240$ points. Here we can routinely run with $N = 1000$ points. Most of the calculations were done with $\Delta s = 0.02$ and s_N chosen much larger, depending on the radius of the ring sink, to ensure good convergence.

5. Results

Computations were performed over a variety of ring sink radii, examples of which can be seen in figures 5 and 7. Firstly, the results were compared with the asymptotic solution to verify the accuracy of the method. Figure 5 shows a comparison with the asymptotic solution for $\rho = 0.5$, $F = 0.3$ and for $\rho = 4$, $F = 1$. Clearly, agreement is good in both cases. The depth of the 'major' dip is slightly underestimated by the asymptotic solution. At smaller values of Froude number, the two methods give solutions that are almost indistinguishable. The formation of the secondary stagnation ring in the full nonlinear solution when $\rho > \sqrt{2}$ was also verified, as illustrated in figure 5. As in the asymptotic solution, the central flat region of the surface became

https://doi.org/10.1017/jfm.2011.551 Published online by Cambridge University Press

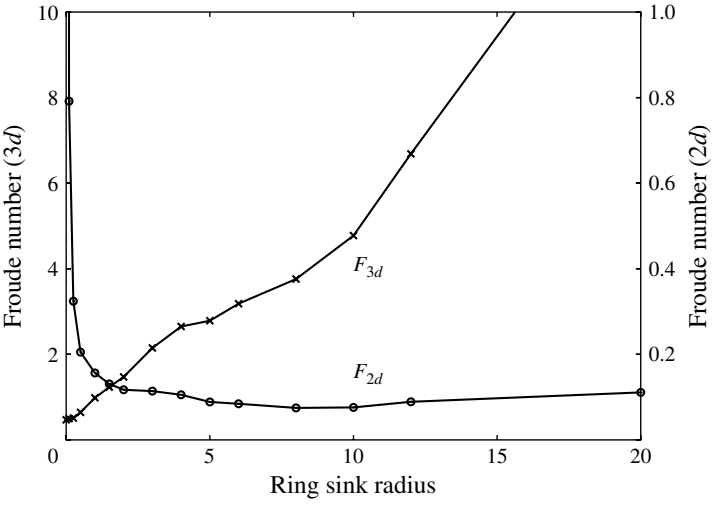


FIGURE 6. Maximum Froude number, F ($\times$), and maximum two-dimensional Froude number, F_2 ($\circ$), for which steady-state solutions exist at different ring sink radii. The curve for F_2 levels off beyond a sink/source radius of around $\rho = 20$.

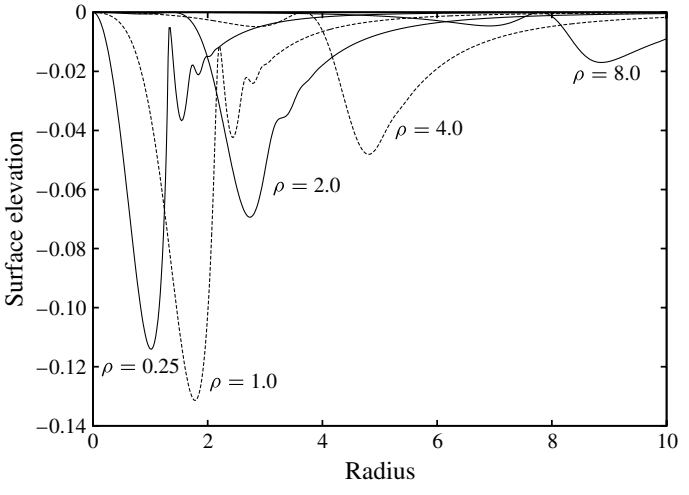


FIGURE 7. Maximum Froude number free surface shapes $z = \eta(r)$ for different ring sink radii. Sink radii $\rho = 0.25, 1, 2, 4, 8$. Froude numbers corresponding to these surfaces are $F = 0.497, 0.983, 1.472, 2.650, 3.760$, all of which are close to the limiting values.

broader as the radius of the sink increased until a small dip appeared as the critical value was passed. In figure 5, this dip can be seen at around $r = 3$ for the case $\rho = 4$.

Following this, a series of calculations was performed in which the maximum steady-state Froude numbers for a range of sink radii were obtained. For each value of the radius, the Froude number was gradually increased until the numerical method no longer converged. Figure 6 shows the maximum value of the Froude number and the equivalent two-dimensional Froude number, F_2, for increasing ring sink radii. The solutions obtained in the limit as $\rho \to 0$ were found to agree with those of the submerged point sink Forbes & Hocking (1990), while as $\rho \to \infty$ the results matched those of a line sink presented by Hocking & Forbes (1991). Interestingly, the value of

https://doi.org/10.1017/jfm.2011.551 Published online by Cambridge University Press

the maximal two-dimensional Froude number, F_2, reaches a minimum as ρ increases, before rising up to the line sink value of $F_2 \approx 0.11$.

It is of interest to examine the shape of the surface as the sink radius increases to determine how the behaviour transitions from the point sink/source-like flows to the line sink/source-like flows. At low sink radius the results proved to be very similar to the original work of Forbes & Hocking (1990) for flow into a point sink. As Froude number increased, a 'wiggle' formed on the outer edge of the dip around the central sink region. This wiggle grew into a bump that eventually rose up near to the stagnation level as the Froude number increased, causing the solution method to fail, see figure 7. In fact, the peak height of this bump, at maximum Froude number, decreased slightly as ρ increased. As an example, the maximum Froude number for the case $\rho = 0.25$ was $F = 0.497$ compared with the value of $F = 0.50$ found by Forbes & Hocking (1990) for the point sink, and the maximum height reached by this bump was slightly below the stagnation level.

As sink radius increased, the maximum Froude number increased, reflecting the lower local sink strength, but the maximum height of this bump decreased, as can be clearly seen in figure 7, which shows maximum Froude number solutions for $\rho = 0.25, 1, 2, 4, 8$. The bump did still appear even after the stagnation ring identified by the asymptotic solution had formed at $\rho = \sqrt{2}$. However, for values of sink radius greater than around $\rho = 3$, the bump no longer formed, making the maximum Froude number flow qualitatively like that due to a line sink.

Another interesting transition occurred at sink radius $\rho = \sqrt{2}$. For values of $\rho < \sqrt{2}$, the magnitude of the deepest dip on the free surface increased as the sink radius increased, but once the sink radius had gone past this value, the maximum dip depth began to decrease (see figure 7).

At very large values of sink radius, the steady solutions appeared to be very similar to the asymptotic solution for all values of Froude number, with the dips on either side of the major stagnation ring (approximately above the sink) simply getting deeper until the solution method failed to converge. The dip that forms inside the secondary stagnation ring grows to become the inner dip inside the stagnation point that forms directly above the ring sink.

While the transition in qualitative behaviour from point-sink-like to line-sink-like occurs at around $\rho \approx 3$, the asymmetry persists to very large values of radius. Figure 8 shows a solution with $\rho = 40$. The solution is beginning to look like the line sink solution described in Hocking & Forbes (1991), but still has the asymmetry in the depth of the inner and outer dips. Despite the fact that the maximum steady-state (two-dimensional) Froude number levelled off at around $\rho = 20$, this asymmetry persists to very large values of ring sink radius, and in fact is well predicted by the two-term approximation in § 3.3, as is evident from figure 4.

6. Conclusions

We have considered the steady flow generated by a ring sink or source submerged beneath a free surface. The problem is of relevance to flows in lakes and reservoirs during withdrawal (or inflow from a single pipe inlet). It has been demonstrated that at low flow rate there is a transition from a single central stagnation point to a situation in which a secondary stagnation ring forms on the surface as the radius of the source/sink passes through $\rho = \sqrt{2}$. This was proved to be true for the asymptotic solution and was confirmed numerically. In the limit as the radius approaches zero, the

https://doi.org/10.1017/jfm.2011.551 Published online by Cambridge University Press

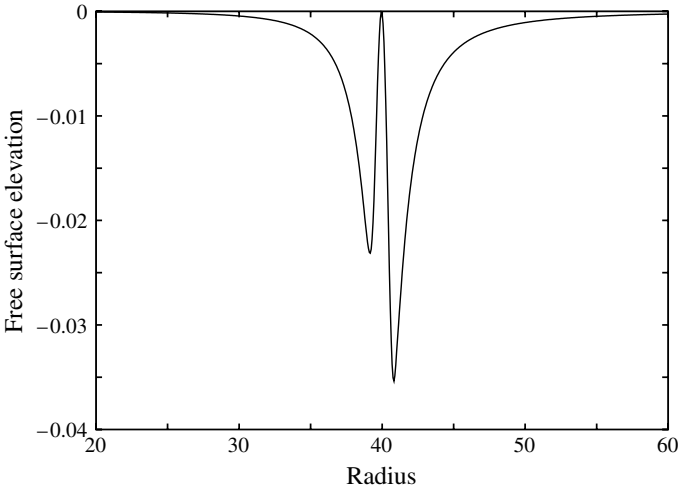


FIGURE 8. Free surface shape at maximum Froude number for ring radius $\rho = 40$.

results approached those of the flow due to a central point source or sink, and as the radius increased the local flow near the ring sink approached that of a line sink.

Critical maximum steady flows have been computed for a range of values of radius of the ring sink and these are shown to be consistent with the limiting line and point sink solutions. The characteristics of the asymptotic solutions were shown to exist in the full nonlinear solutions. In addition, the transition in behaviour from point-like to line-like was demonstrated at the maximum values of flow rate. The apparent cause of the breakdown of solutions in the case of a point sink (formation of a bump that rose to the stagnation level), demonstrated in Forbes & Hocking (1990), was shown to persist as the point sink became a ring sink, but decreased in intensity until it was no longer evident when the sink radius became about three times its depth. While the transition in behaviour occurs at quite a small value of radius ρ, the asymmetry in the surface shape persists to very large values.

The conclusions we can draw from this work in the context of the selective withdrawal problem are not clear. The work shows how and for which parameter values the point sink solutions change behaviour to approximate the behaviour of a two-dimensional withdrawal flow, but they do not provide any clearer reason for the breakdown of the line sink flows. By approaching the line sink case from a different perspective, they do confirm the results of earlier work, however, and suggest that it is a real effect rather than an artifact of the numerical methods being employed. These results, in combination with past work and future unsteady calculations, may shed light on this important problem.

Appendix A. Deriving $G(\bar{r})$ in terms of special functions

Noting that the integrand of $G(\bar{r})$, (3.7), is even, we may write

$$G(\bar{r}) = 2\int_0^{\pi} \frac{\bar{r} - \cos\theta}{\left(1 + \bar{r}^2 + \dfrac{1}{\rho^2} - 2\bar{r}\cos\theta\right)^{3/2}}\,\mathrm{d}\theta. \tag{A 1}$$

https://doi.org/10.1017/jfm.2011.551 Published online by Cambridge University Press

Introducing a new variable u satisfying $u^2 = 1 + \bar{r}^2 + 1/\rho^2 - 2\bar{r}\cos\theta > 0$, it is a straightforward if laborious process to show that

$$G(\bar{r}) = \frac{2}{\bar{r}} \int_p^q \frac{[(\bar{r}^2 - 1 - 1/\rho^2) + u^2]}{u^2\sqrt{(u^2 - p^2)(q^2 - u^2)}}\,\mathrm{d}u$$
$$= \frac{2(\bar{r}^2 - 1 - 1/\rho^2)}{\bar{r}} I_1(p, q) + \frac{2}{\bar{r}} I_2(p, q), \tag{A 2}$$

where $p = \sqrt{(1 - \bar{r})^2 + 1/\rho^2}$ and $q = \sqrt{(1 + \bar{r})^2 + 1/\rho^2}$, and

$$I_1 = \int_p^q \frac{\mathrm{d}u}{u^2\sqrt{(u^2 - p^2)(q^2 - u^2)}}, \tag{A 3}$$

$$I_2 = \int_p^q \frac{\mathrm{d}u}{\sqrt{(u^2 - p^2)(q^2 - u^2)}}. \tag{A 4}$$

We now proceed as in the appendix of Forbes & Hocking (1990). Considering first I_2, and making a change of variable to t, where $t^2 = (q^2 - u^2)/(q^2 - p^2)$, after some algebra we obtain

$$I_2 = \frac{1}{q} \int_0^1 \frac{\mathrm{d}t}{\sqrt{(1 - t^2)\left(1 - \left(\dfrac{q^2 - p^2}{q^2}\right) t^2\right)}}$$
$$= \frac{1}{q} K\left(\frac{q^2 - p^2}{q^2}\right), \tag{A 5}$$

where $K(\zeta)$ is the complete elliptic integral of the first kind, as on page 590 of Abramowitz & Stegun (1970), and $\zeta = 1 - (p/q)^2 = 4\bar{r}\left((1 + \bar{r})^2 + 1/\rho^2\right)^{-1}$.

Similarly, in considering I_1, we change the variable to t, where, this time, $t^2 = q^2(u^2 - p^2)/u^2(q^2 - p^2)$, and again after some algebra we obtain

$$I_1 = \frac{1}{p^2 q} \int_0^1 \frac{\sqrt{1 - \left(\dfrac{q^2 - p^2}{q^2}\right)}}{\sqrt{1 - t^2}}\,\mathrm{d}t$$
$$= \frac{1}{p^2 q} E\left(\frac{q^2 - p^2}{q^2}\right), \tag{A 6}$$

where $E(\zeta)$ is the complete elliptic integral of the second kind.

Appendix B. Proof of theorem 1

Proof. Noting that $q^2 - p^2 = 4\bar{r}$, we see that $G(\bar{r}) = 0$ when

$$\frac{E(\zeta)}{K(\zeta)} = \frac{(1 - \bar{r})^2 + 1/\rho^2}{1 - \bar{r}^2 + 1/\rho^2} = \Theta. \tag{B 1}$$

To prove this result, we build a picture of $E(\zeta)/K(\zeta)$ and $\Theta = ((1 - \bar{r})^2 + 1/\rho^2)/(1 - \bar{r}^2 + 1/\rho^2)$ as functions of $\bar{r}$, beginning with Θ.

https://doi.org/10.1017/jfm.2011.551 Published online by Cambridge University Press

Consider first the right-hand side of (B 1), denoted by Θ. Note that Θ is positive so long as $\bar{r}^2 < 1 + 1/\rho^2$ and increases to infinity as $\bar{r} \to \sqrt{1 + 1/\rho^2}$. Also, $\Theta = 1$ when $\bar{r} = 0, 1$ and $\Theta < 1$ when $0 < \bar{r} < 1$. On the other hand, for $\bar{r} > \sqrt{1 + 1/\rho^2}$, $\Theta < 0$.

Now consider $E(\zeta)/K(\zeta)$ on the left-hand side of (B 1). It is not difficult to show that $0 < \zeta < 1$ for all $\bar{r}$. Further calculation shows that ζ is monotone decreasing for $0 < \bar{r} < \sqrt{1 + (1/\rho^2)}$. Moreover, $E(\zeta)/K(\zeta)$ decreases monotonically from 1 at $\zeta = 0$ (that is, $\bar{r} = 0$) to 0 as $\zeta \to 1$ (that is, $\bar{r} \to \infty$).

So, aside from at $\bar{r} = 0$, the curves defined by Θ and $E(\zeta)/K(\zeta)$ viewed as functions of $\bar{r}$ can intersect in at most one further place. To see this, consider derivatives at $\bar{r} = 0$. The series expansions for E, K as on page 591 of Abramowitz & Stegun (1970) yield

$$E \approx \frac{\pi}{2}\left(1 + \frac{1}{4}\zeta + \frac{9}{64}\zeta^2 + O(\zeta^3)\right), \tag{B 2}$$

$$K \approx \frac{\pi}{2}\left(1 - \frac{1}{4}\zeta - \frac{3}{64}\zeta^2 + O(\zeta^3)\right). \tag{B 3}$$

Now

$$\frac{\mathrm{d}(E/K)}{\mathrm{d}\bar{r}} = \frac{\mathrm{d}(E/K)}{\mathrm{d}\zeta} \cdot \frac{\mathrm{d}\zeta}{\mathrm{d}\bar{r}} \tag{B 4}$$

and

$$\frac{\mathrm{d}^2(E/K)}{\mathrm{d}\bar{r}^2} = \frac{\mathrm{d}(E/K)}{\mathrm{d}\zeta} \cdot \frac{\mathrm{d}^2\zeta}{\mathrm{d}\bar{r}^2} + \frac{\mathrm{d}^2(E/K)}{\mathrm{d}\zeta^2} \cdot \left(\frac{\mathrm{d}\zeta}{\mathrm{d}\bar{r}}\right)^2, \tag{B 5}$$

and the truncated series can be used to compute $\mathrm{d}(E/K)/\mathrm{d}\zeta$ and $\mathrm{d}^2(E/K)/\mathrm{d}\zeta^2$ exactly at $\bar{r} = 0$, with $\mathrm{d}\zeta/\mathrm{d}\bar{r}$ and $\mathrm{d}^2\zeta/\mathrm{d}\bar{r}^2$ directly calculable. These first and second derivatives of E/K with respect to $\bar{r}$ may be computed exactly at $\bar{r} = 0$.

Similarly, both $\mathrm{d}\Theta/\mathrm{d}\bar{r}$ and $\mathrm{d}^2\Theta/\mathrm{d}\bar{r}^2$ may be computed directly and evaluated at $\bar{r} = 0$. The task is straightforward for *Maple*, which reveals that at $\bar{r} = 0$,

$$\frac{\mathrm{d}(E/K)}{\mathrm{d}\bar{r}} = \frac{-2}{1 + 1/\rho^2} = \frac{\mathrm{d}\Theta}{\mathrm{d}\bar{r}}, \tag{B 6}$$

so the two functions of $\bar{r}$ have identical slopes there. In order to decide whether there is a second place where the two expressions in (B 1) are equal, for some $\bar{r} > 0$, it is therefore necessary to consult the second derivatives. *Maple* shows that

$$\frac{\mathrm{d}^2\Theta}{\mathrm{d}\bar{r}^2} = \frac{4}{1 + 1/\rho^2} \quad \text{and} \quad \frac{\mathrm{d}^2(E/K)}{\mathrm{d}\bar{r}^2} = \frac{6}{(1 + 1/\rho)^2}. \tag{B 7}$$

Both second derivatives are therefore positive at $\bar{r} = 0$. Given the trajectories of the two curves for $\bar{r} > 0$, simple geometry shows that for a second zero to exist, the curvature of the plot of E/K against $\bar{r}$ must be greater at $\bar{r} = 0$ than that of Θ against $\bar{r}$, in other words,

$$\frac{6}{(1 + 1/\rho)^2} > \frac{4}{1 + 1/\rho^2}. \tag{B 8}$$

https://doi.org/10.1017/jfm.2011.551 Published online by Cambridge University Press

However,

$$\frac{6}{(1+1/\rho)^2} - \frac{4}{1+1/\rho^2} = \frac{2(\rho^2-2)\rho^2}{(\rho^2+1)^2} > 0 \tag{B 9}$$

whenever $\rho^2 > 2$, that is, $\rho > \sqrt{2}$, as required. □

REFERENCES

ABRAMOWITZ, M. & STEGUN, I. A. 1970 *Handbook of Mathematical Functions*. Dover.

CRAYA, A. 1949 Theoretical research on the flow of nonhomogeneous fluids. *La Houille Blanche* **4**, 44–55.

FORBES, L. K. & HOCKING, G. C. 1990 Flow caused by a point sink in a fluid having a free surface. *J. Austral. Math. Soc.* B **32**, 231–249.

FORBES, L. K. & HOCKING, G. C. 1993 Flow induced by a line sink in a quiescent fluid with surface-tension effects. *J. Austral. Math. Soc. Ser.* B **34**, 377–391.

FORBES, L. K. & HOCKING, G. C. 2003 On the computation of steady axi-symmetric withdrawal from a two-layer fluid. *Comput. Fluids* **32**, 385–401.

FORBES, L. K., HOCKING, G. C. & CHANDLER, G. A. 1996 A note on withdrawal through a point sink in fluid of finite depth. *J. Austral. Math. Soc. Ser.* B **37**, 406–416.

HARLEMAN, D. R. F. & ELDER, R. E. 1965 Withdrawal from two-layer stratified flow. *J. Hydraul. Div. ASCE* **91** (4), 43–58.

HOCKING, G. C. 1985 Cusp-like free-surface flows due to a submerged source or sink in the presence of a flat or sloping bottom. *J. Austral. Math. Soc. Ser.* B **26**, 470–486.

HOCKING, G. C. 1991 Withdrawal from two-layer fluid through line sink. *J. Hydraul. Engng ASCE* **117** (6), 800–805.

HOCKING, G. C. 1995 Supercritical withdrawal from a two-layer fluid through a line sink. *J. Fluid Mech.* **297**, 37–47.

HOCKING, G. C. & FORBES, L. K. 1991 A note on the flow induced by a line sink beneath a free surface. *J. Austral. Math. Soc. Ser.* B **32**, 251–260.

HOCKING, G. C. & FORBES, L. K. 2001 Supercritical withdrawal from a two-layer fluid through a line sink if the lower layer is of finite depth. *J. Fluid Mech.* **428**, 333–348.

HOCKING, G. C., VANDEN BROECK, J.-M. & FORBES, L. K. 2002 Withdrawal from a fluid of finite depth through a point sink. *ANZIAM J.* **44**, 181–191.

HUBER, D. G. 1960 Irrotational motion of two fluid strata towards a line sink. *J. Engng. Mech. Div. Proc. ASCE* **86** (EM4), 71–85.

IMBERGER, J. & HAMBLIN, P. F. 1982 Dynamics of lakes, reservoirs and cooling ponds. *Annu. Rev. Fluid Mech.* **14**, 153–187.

IMBERGER, J. & PATTERSON, J. C. 1990 Physical limnology. In *Advances in Applied Mechanics* (ed. J. W. Hutchinson & T. Wu). vol. 27. pp. 303–475. Academic.

JIRKA, G. H. 1979 Supercritical withdrawal from two-layered fluid systems. Part 1. Two-dimensional skimmer wall. *J. Hydraul. Res.* **17** (1), 43–51.

JIRKA, G. H. & KATAVOLA, D. S 1979 Supercritical withdrawal from two-layered fluid systems. Part 2. Three dimensional flow into a round intake. *J. Hydraul. Res.* **17** (1), 53–62.

LUBIN, B. T. & SPRINGER, G. S. 1967 The formation of a dip on the surface of a liquid draining from a tank. *J. Fluid Mech.* **29**, 385–390.

MEKIAS, H. & VANDEN-BROECK, J.-M. 1991 Subcritical flow with a stagnation point due to a source beneath a free surface. *Phys. Fluids* A **3**, 2652–2658.

PEREGRINE, H. 1972 A line source beneath a free surface. *Rep.* 1248. Mathematics Research Center, University of Wisconsin, Madison.

SAUTREAUX, C. 1901 Mouvement d'un liquide parfait soumis à lapesanteur. Dé termination des lignes de courant. *J. Math. Pures Appl.* **7** (5), 125–159.

STOKES, T. E., HOCKING, G. C. & FORBES, L. K. 2002 Unsteady free surface flow induced by a line sink. *J. Engng Maths* **47**, 137–160.

https://doi.org/10.1017/jfm.2011.551 Published online by Cambridge University Press

STOKES, T. E., HOCKING, G. C. & FORBES, L. K. 2005 Unsteady flow induced by a withdrawal point beneath a free surface. *ANZIAM J.* **47**, 185–202.

TUCK, E. O. 1975 On air flow over free surfaces of stationary water. *J. Austral. Math. Soc. Ser.* B **19**, 66–80.

TUCK, E. O. & VANDEN BROECK, J.-M. 1984 A cusp-like free surface flow due to a submerged source or sink. *J. Austral. Math. Soc. Ser.* B **25**, 443–450.

TYVAND, P. A. 1992 Unsteady free-surface flow due to a line source. *Phys. Fluids* A **4**, 671–676.

VANDEN BROECK, J.-M. & KELLER, J. B. 1987 Free surface flow due to a sink. *J. Fluid Mech.* **175**, 109–117.

VANDEN BROECK, J.-M., SCHWARTZ, L. W. & TUCK, E. O. 1978 Divergent low-Froude-number series expansion of nonlinear free-surface flow problems. *Proc. R. Soc. Lond. Ser.* A **361**, 207–224.

WOOD, I. R. & LAI, K. K. 1972 Selective withdrawal from a two-layered fluid. *J. Hydraul. Res.* **10** (4), 475–496.

XUE, X. & YUE, D. K. P 1998 Nonlinear free-surface flow due to an impulsively started submerged point sink. *J. Fluid Mech.* **364**, 325–347.

https://doi.org/10.1017/jfm.2011.551 Published online by Cambridge University Press